

Coupling between Edge and Bulk in Strong-Field Quantum Dots

S.-R. Eric Yang^{a,b}, and A.H. MacDonald^b

^a Department of Physics, Korea University, Seoul, Korea

^b Department of Physics, University of Texas at Austin, Austin, TX 78712, USA

(October 26, 2018)

The maximum-density-droplet (MDD) state of quantum-dot electrons becomes unstable at strong magnetic fields to the addition of interior holes. Using exact diagonalization, we demonstrate that the first hole is located at the center of the dot when the number of electrons N is smaller than ~ 14 and is located away from the center for larger dots. The separation between field strengths at which additional holes are introduced becomes small for large dots, explaining recent observations of a rapid increase in dot area when the magnetic field is increased beyond the MDD stability limit. We comment on correlations between interior hole and collective edge fluctuations, and on the implications of these correlations for edge excitation models in bulk systems.

PACS numbers: 75.50.Pp, 75.10.-b, 75.30.Hx

The fabrication of quantum dots has now reached an advanced state in which the shape of the confinement potential and the number of electrons in a dot can be tuned precisely [1]. In a strong magnetic field, quantum dots display a number of interesting many body effects [2–5], closely related to those exhibited by bulk two-dimensional (2D) electron systems in the quantum Hall regime. Correlation effects become strong because the single-particle level spacing in this limit is small compared to the typical Coulomb interaction energy scale. Some time ago we [6] predicted that quantum dots in a strong magnetic field would form a *maximum density droplet* state with approximately uniform electron density, close to that of a 2D system with a single filled Landau level ($\rho_0 = (2\pi\ell^2)^{-1}$ where $\ell = (\hbar c/eB)^{1/2}$ is the magnetic length), that would be stable over a wide field range. Indeed, features associated with the wide MDD state stability interval are prominent in *addition potential vs. magnetic field* traces measured [7–9] by using transport resonances to track the gate voltages at which electrons are added to a quantum dot. The MDD state is a finite-size precursor and shares many attributes with bulk $\nu = 1$ quantum Hall ferromagnet [10,11] states. With increasing magnetic field, ρ_0 increases and Coulomb interactions eventually make the MDD state unstable, favoring a state in which the average electron density is lowered. Reimann *et al.* have concluded [12], on the basis of spin-density-functional calculations, that in large dots the density is first lowered by an edge reconstruction similar to those that occur in bulk systems at integer [13,14] and fractional [15] filling factors. In their self-consistent field calculations the MDD state evolves into a state with a modulation of charge density along the edge and a ring of electron density that break off from the uniform density droplet. For smaller dots, on the other hand, MacDonald *et al.* have shown [6] that the average density is lowered by introducing holes close to the center of the droplet.

This Rapid Communication is motivated by recent experiments [8] of Oosterkamp *et al.*, who have measured *addition potential vs. magnetic field* traces for quantum dots containing 0 to 40 electrons. These authors find that for N larger than about 15, the area occupied by the quantum dot electron cloud increases rapidly on the high-field side of the MDD stability region. We have investigated the quantum dot phase diagram by performing exact diagonalization calculations, assuming Zeeman fields large enough to ensure full spin polarization. We find that holes are added to the interior of the dots with increasing field, increasing the electron cloud area; for $N > N_c$ ($N_c \approx 13 - 14$) the interior holes stay away from the center of the dot, while for $N < N_c$ the holes form a puddle at the center of the dot. The phase diagram we obtain for hole number *vs.* field, is in qualitative agreement with experimental data. We find that the rate at which holes are added with field increases for larger dots, explaining the observations of Oosterkamp *et al.* We also find that correlations develop between the motion of holes in the interior of the dot and collective edge excitations of the dot, and discuss the nature of the corresponding coupling in bulk integer filling factor quantum Hall systems.

We consider a system of 2D electrons confined by a parabolic potential, $V(r) = m^*\Omega^2 r^2/2$. and confine our attention here to the strong magnetic field limit, $\Omega/\omega_c \ll 1$. ($\omega_c = eB/m^*c$, where B is the magnetic field perpendicular to the 2D layer.) In this limit the symmetric gauge single-particle eigenstates in the lowest Landau level [16] are conveniently classified by an angular momentum index $m \geq 0$:

$$\epsilon_m = \hbar\omega_c/2 + \gamma(m+1), \quad (1)$$

where $\gamma = m\Omega^2\ell^2$. We will drop the constant kinetic energy from subsequent discussion. The Hamiltonian is invariant under spatial rotations about the axis that is perpendicular to the 2D plane and passes through the center

of the dot. It follows that the total angular momentum M_z is a good quantum number. The Hamiltonian of the dot in the fully spin-polarized, lowest-Landau-level, Hilbert space is

$$H = \sum_m \gamma(m+1)c_m^\dagger c_m + \frac{1}{2} \sum_{m'_1, m'_2, m_1, m_2} \langle m'_1 m'_2 | V | m_1 m_2 \rangle c_{m'_1}^\dagger c_{m'_2}^\dagger c_{m_2} c_{m_1}. \quad (2)$$

The characteristic energy for the two-particle Coulomb matrix elements is $e^2/\epsilon\ell$, where ϵ is the host semiconductor dielectric constant. The eigenstates of this Hamiltonian depend only on the dimensionless ratio between the two competing terms, $\tilde{\gamma} = \gamma/(e^2/\epsilon\ell)$. The MDD state is the eigenstate of this Hamiltonian with the minimum angular momentum allowed by the Pauli exclusion principle, $M_z \rightarrow M_z^{MDD} = N(N-1)/2$, and is the ground state of this Hamiltonian for strong confinement (large $\tilde{\gamma}$). We find it useful below to denote occupation number eigenstates by lists ordered by increasing angular momentum. For example, in this notation the $N = 4$ MDD state is $(\bullet, \bullet, \bullet, \bullet, \circ, \circ, \dots)$, where the symbols \bullet and \circ denote occupied and unoccupied single-particle states.

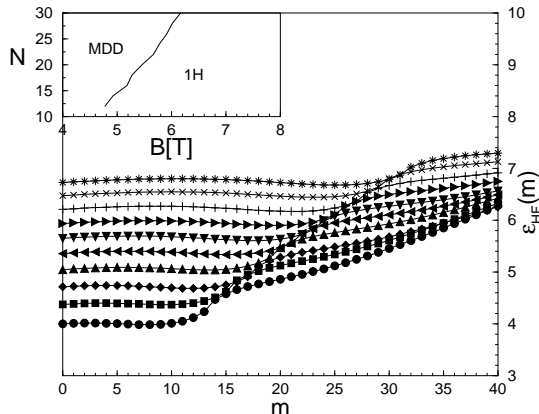


FIG. 1. Hartree-Fock quasi-particle energies $\epsilon_{HF}(m)$ of the MDD state as a function of m for different values of N . $\tilde{\gamma}$ is chosen, for each N , so that the MDD is close to its instability point; $\tilde{\gamma} = 0.077, 0.08, 0.082, 0.085, 0.0875, 0.0925, 0.0975, 0.1, 0.108, 0.113$ for $N = 30, 28, 26, \dots, 14, 12$, respectively. The inset displays the HF phase boundary between the MDD state and one-hole states for a dot with $\hbar\Omega = 3\text{meV}$. The dimensionless confinement strength parameter $\tilde{\gamma}$, the field in Tesla B , and the confinement oscillator frequency in meV are related by $B[\text{Tesla}] = [0.131(\hbar\Omega[\text{meV}])^2/\tilde{\gamma}]^{2/3}$.

In Fig. 1 we have plotted Hartree-Fock quasiparticle energies $\epsilon_{HF}(m)$, for $m = 0$ to $m = 40$ for MDD states with $N = 12, 14, \dots, 28, 30$. ($\epsilon_{HF}(m) = \gamma(m+1) + \sum_{m'=0}^{N-1} U_{m,m'}$ where $U_{m,m'} = \langle mm' | V | mm' \rangle - \langle mm' | V | m'm \rangle$) The confinement strengths used in these

plots are, for each N , near the MDD stability limit. In HF theory, the MDD becomes unstable when an unoccupied interior quasiparticle energy exceeds the edge quasiparticle energy, *i.e.* when $\epsilon_{HF}(m^*) > \epsilon_{HF}(N-1)$ for $m^* < N-1$. We see from Fig. 1 that holes are first introduced near the center of the dot $N \leq 12$ and gradually move outward as N increases. This qualitative prediction of Hartree-Fock theory is generally confirmed by the exact diagonalization calculations we discuss below.

To understand the role played by correlations we first discuss a small dot for which an accurate analytic calculation is possible. For $N = 3$ the MDD has $M_z^{MDD} = 3$ and HF theory predicts that when γ is reduced the first hole is introduced in the $m^* = 0$ state, increasing the $N = 3$ ground state angular momentum to $M_z = 6$. The exact single hole ground state is obtained by diagonalizing the many-particle Hamiltonian in the space of states with $M_z = 6$. Fig. 1 suggests that the probability of occupying single-particle states with large m is small, since quasiparticle energies increase rapidly outside the MDD. If we can neglect the possibility of occupying states with $m > m_c = 4$, the only additional state in the Hilbert space with $M_z = 6$ has the interior hole at $m = 1$ rather than $m = 0$ and excites an edge magnetoplasmon at the edge [6,18] by making a particle-hole excitation from $m = 3$ to $m = 4$. The many-particle Hamiltonian matrix in this two-dimensional Hilbert space is

$$\begin{pmatrix} 9\gamma + U_{1,2} + U_{1,3} + U_{2,3} & U_{0413} \\ U_{0413} & 9\gamma + U_{0,2} + U_{0,4} + U_{2,4} \end{pmatrix}, \quad (3)$$

where

$$U_{m_1 m_2 m_3 m_4} = \langle m_1 m_2 | V | m_3 m_4 \rangle - \langle m_1 m_2 | V | m_4 m_3 \rangle. \quad (4)$$

The interaction contributions to the matrix elements in Eq. 3 in $e^2/\epsilon\ell$ units are 0.940 and 1.114 respectively along the diagonal and 0.083 in the off-diagonal term. The off diagonal term introduces correlation between hole motion and collective edge excitations in this small dot, reducing the ground state energy to $9\gamma + 0.907e^2/\epsilon\ell$. The $N = 3$ ground state energy, in this approximation, is $9\gamma + 0.907e^2/\epsilon\ell$, compared to the MDD state energy which is $6\gamma + 1.204e^2/\epsilon\ell$. Note that correlations between bulk and edge shift the MDD stability limit from $\tilde{\gamma} = 0.088$ in the Hartree-Fock approximation to $\tilde{\gamma} = 0.099$. An exact diagonalization for $N = 3$ confirms the accuracy of this Hilbert space truncation.

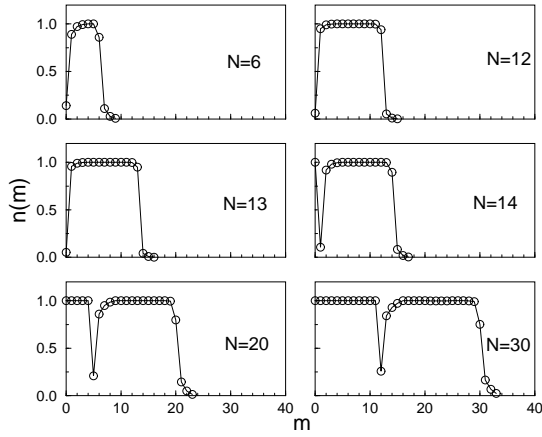


FIG. 2. Occupation number distributions for the one-hole MDD states of $N = 6, 12, 13, 14, 20, 30$ quantum dots.

Fig. 2 summarizes our numerical exact diagonalization results for one hole states at larger N by plotting mean-occupation numbers for all single-particle states. For $N = 6$, the HF approximation places the hole at $m^* = 0$, yielding a total $M_z = 21$. The exact single-hole state occurs at the same value of M_z , but the hole position and the dot edge have correlated quantum fluctuations, evidenced in Fig. 2 by the finite probability for finding the hole in the $m = 1$ state. Equal time correlation functions, not illustrated here, demonstrate that the hole has a higher probability of being on the same side of the system as edge density modulations. For $N = 12$, we again find that the exact single-hole state has the same M_z as the Hartree-Fock state with $m^* = 0$, $M_z = 78$, and correlated bulk-hole edge excitations. This pattern continues for larger particle numbers with the nominal hole angular momenta moving out at larger N . For $N = 30$, for example, the nominal angular momentum of the single-hole is $m^* = 12$. Note that the hole angular momentum has fluctuations only to the high-angular momentum side of its nominal value. This property is a combined consequence of angular momentum conservation and the chiral [19] nature of the collective edge excitations with which it is correlated. The one-hole nominal locations for $N = 6, 12, 13, 14, 20, 30$ $m^* = 0, 0, 0, 1, 5, 12$ respectively. The total hole occupation number determined by summing the depleted occupation numbers inside the quantum dots in Fig. 2 is accurately quantized at 1, demonstrating that holes and edge excitations are correlated but that charge fluctuations from bulk to edge or *vice versa* is negligible.

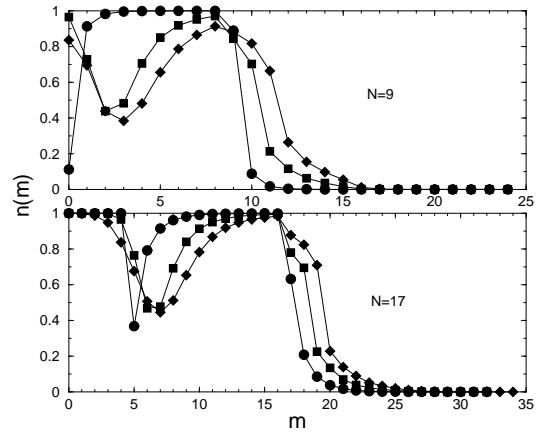


FIG. 3. Occupation number distributions for one-hole (circle), two-hole (square), and three-hole (diamond) MDD states for $N = 9$ and $N = 17$.

For each particle number N , the number of holes in the ground state increases as $\tilde{\gamma}$ decreases, with the number of bulk holes accurately conserved to larger hole numbers for larger N . In Fig. 3, we plot occupation number distributions for the one-hole two-hole and three-hole states at $N = 9$ and $N = 17$. We find that the average number of interior holes in the nominal two and three hole states deviates from integer values by 0.007 and 0.05 for $N = 9$ and 0.003 and 0.006 for $N = 17$, demonstrating accurate interior hole-number conservation. The one-hole and two-hole M_z values are 45 and 50 for $N = 9$ and 148 and 158 for $N = 17$, giving nominal first-hole and second-hole m^* values of 0 and 4 for $N = 9$ and 5 and 7 for $N = 17$. It is clear from Fig. 3, however, that correlations within the two-hole system make these assignments, based on the sequence of ground state angular momenta values, less meaningful. For States with two or more holes, correlations among the holes and correlations between the holes and the edge system are both important.

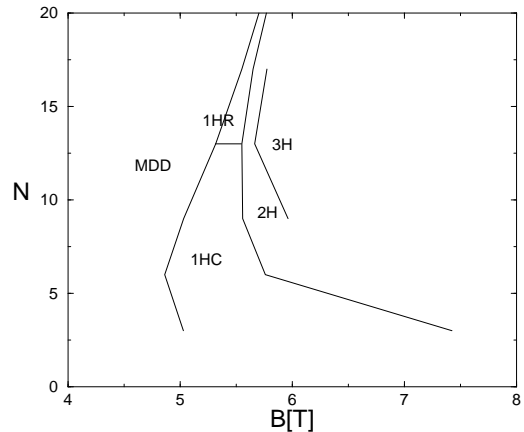


FIG. 4. Phase diagram near the stability limit of the MDD state. The symbol MDD stands for the maximum density droplet, while 1HC and 1HR represent respectively centered ($m^* = 0$) and ring ($m^* > 0$) single-hole states. 2H and 3H represent states with two and three holes. States with more than three holes have not been studied but will occur at larger fields. Classifying states near the MDD limit by the number of holes is meaningful when charge fluctuations between the interior of the MDD and its edge are negligible.

To facilitate comparison with experiment, we have plotted a phase diagram of MDD related states in Fig.4 *vs.* particle number N and field, parameters that are known experimentally, using a typical value for the parabolic confinement strength $\hbar\Omega = 3meV$. We have not considered states with more than three holes because of the growing difficulty of carrying out accurate exact diagonalization calculations, and expect that the region at the top right of this phase diagram should be occupied by states with four and more interior holes. Note that the spacing in field between hole number addition points becomes small for large dots, explaining the sudden increase in quantum dot area observed by Oosterkamp *et al.*. The stability regime of multiple hole states is seriously underestimated by Hartree-Fock and density-functional-theory calculations which are unable to account for the strong correlations possible in the quantum Hall regime.

The sign of cusps in the magnetic field dependence of the addition spectrum contains valuable information about the shape of the phase boundaries. Oosterkamp *et al* [8] measured is the magnetic field dependence of the addition spectrum given by $\mu_N = E_N - E_{N-1} + \hbar\omega_c/2$, where $E_N = \gamma(N + M_z) + U(N, M_z)$ is the groundstate energy of an N -electron system. (Here $U(N, M_z)$ is the total interaction energy). As the applied magnetic field increases, groundstate level crossings in the $N - 1$ and N particle systems lead to positive and negative cusps [3], respectively. For $N > 8$ the phase boundary between the MDD and one-hole states is an increasing function of magnetic field (see Fig.4). This implies that the $N - 1$ -electron dot will cross the phase boundary before the N -electron dot does. The measured upward cusps are consistent with this expectation. Upward cusps are also seen between one-hole and two-hole states.

The strong correlations that we find between interior holes and the edge excitations of quantum dots also applies to bulk quantum Hall systems. These correlations are important because of the long-range of the Coulomb interaction, which causes charge fluctuations in the two subsystems to interact strongly. Recent scanning probe studies of 2D electron systems in the quantum Hall regime [20] have made it clear that real experimental samples always have low-energy interior hole and electron low-energy degrees of freedom. At low temperatures charge carriers in the bulk are localized so these

disorder induced degrees of freedom do not influence the quantum Hall effect. They may, however, influence other properties of the chiral edge state system. Collective excitations at the edge, will induce electric potentials in the interior that will excite the localized hole system. Similar effects cause semiclassical edge magnetoplasmon [21] excitations to be influenced by the bulk conductivity. The possible importance, at experimental temperature and voltage scales, of these interactions for the tunneling density-of-states [22] and other properties measured at the edge deserves more careful consideration.

We are indebted to D.G. Austing and S. Tarucha for valuable discussions. This work was supported by the National Science Foundation under grant DMR0115947, by the Welch foundation, and by the Korea Research Foundation under Grant KRF-2000-015-DP0125.

-
- [1] For recent reviews see L.P. Kouwenhoven, D.G. Austing, and S. Tarucha, Rep.Prog. Phys. **64**, 701 (2001); L.P. Kouwenhoven and P.L. McEuen, in Nano Science and Technology, edited by G.Timp (to be published); H. van Houten, C.W. Beenakker, and A.A.M. Staring, in Single Charge Tunneling, edited by H. Grabert and M.H. Devoret (Plenum, New York, 1992); D.V. Averin and K.K. Likharev, in Mesoscopic Phenomena in Solids, edited by B.L. Altshuler, P. A. Lee, and Webb (Elsevier, Amsterdam, 1991); M.A.Kastner, Rev. Mod.Phys. **64**, 849 (1992); Phys. Today **46** (1),24 (1993).
 - [2] P. A. Maksym and T. Chakraborty, Phys. Rev. Lett. **65**,108 (1990).
 - [3] S.-R. Eric Yang, A. H. MacDonald, M.D. Johnson, Phys. Rev. Lett. **71**, 3195 (1993).
 - [4] S. Tarucha, D.G. Austing, W.G. van der Wiel, L.P. Kouwenhoven, Phys. Rev. Lett. **84**, 2485 (2000).
 - [5] J.J. Palacios, L. Martin-Moreno, G. Chiappe,, E. Louis, and C. Tejedor, Phys. Rev.B **50**, 5760 (1994).
 - [6] A. H. MacDonald, S.-R. Eric Yang, and M.D. Johnson, Aust. J. Phys. **46** 345 (1993); S.-R. Eric Yang, A.H. MacDonald, and M.D. Johnson, Phys. Rev. Lett. **71**, 3194 (1993).
 - [7] R. Ashoori *et al*, Phys. Rev. Lett. **68**, 3088 (1992); R. Ashoori *et al*, Phys. Rev. Lett. **71**, 613 (1993); Nature (London) **379**, 413 (1996).
 - [8] T. H. Oosterkamp, J. W. Janssen, L.P. Kouwenhoven, D. G. Austing, T. Honda, and S. Tarucha, Phys. Rev. Lett. **82**, 2931 (1999). **46**, 345 (1993).
 - [9] O. Klein, C.D. Chamon, D. Tang, D.M. Abuschmagder, U. Meirav, X.G. Wen, M.A. Kastner, S.J. Wind, Phys. Rev. Lett. **74**, 785 (1995).
 - [10] S.L. Sondhi, A. Karlhede, and S.A. Kivelson, Phys. Rev. B **47** 16419 (1993).
 - [11] For a general discussion of integer filling factor quantum Hall ferromagnets see T. Jungwirth and A.H. MacDonald, Phys. Rev. B **63**, 5305 (2001).

- [12] S.M. Reimann, M. Koskinen, M. Manninen, and B.R. Mottelson, Phys. Rev. Lett. **83**, 3270 (1999).
- [13] C.de. C. Chamon and X.G. Wen, Phys. Rev. **49**, 8227 (1994).
- [14] A. Karlhede, et al, Phys. Rev. Lett. **77**, 2061 (1996).
- [15] Xin Wan, Kun Yang, and E.H. Rezayi, cond-mat/0106386.
- [16] Corrections to the lowest Landau level approximation do have quantitative importance in typical experimental circumstances, but are not important for the issues we discuss here. See for example S. Siljamäki *et al.*, cond-mat/0123243.
- [17] V. Gudmundsson and J.J. Palacios, Phys. Rev. B **52**, 11266 (1995).
- [18] U. Zulicke, and A.H. MacDonald Phys. Rev. B **54**, 16813 (1996).
- [19] X.-G. Wen, Int. J. Mod. Phys. **6**, 1711 (1992).
- [20] M.A. Eriksson *et al.* Appl. Phys. Lett. **69**, 671 (1996); S. H. Tessmer *et al.* Nature **392**, 51 (1998); K. L. McCormick *et al.* Phys. Rev. B **59**, 4654 (1999); N. B. Zhitenev *et al.* Nature **404**, 473 (2000).
- [21] V.A. Volkov and S.A. Mikhailov, Zh. Eksp. Teor. Fiz. **98**, 217 (1988).
- [22] C.L. Kane and M.P.A. Fisher, Phys. Rev. Lett. **68**, 1220 (1992).